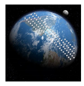

A Reversible Mid-Stratospheric Architecture To Reduce Insolation:

Calculation Details and Data for the Paper

Narayanan M. Komerath and Ravi Deepak
Taksha Institute, Virginia, USA

June 14, 2023

Disclaimer

Work presented is that of the participants and believed to be accurate.

Copyright

Table of Contents

1 Summary

This document presents essential calculations and data that are used in the paper whose title is given in the document title. The first section deals with Uncertainty in various aspects. The next shows the essential elements in designing High Altitude Long Endurance aerodynamic vehicles that must glide through the night without power, staying as high as possible. The third gives data used to construct a roadmap to deploy Flying Leaf vehicles to reduce Earth's Energy Imbalance towards the level of 1990, by 2055. The fourth presents the data used to derive an equivalence between Carbon Emission Units (CEUs or Carbon Credits), and the creditable activities in reflecting sunlight, and towards the UN Sustainable Goals. The fifth shows initial calculations behind the Polar Necklace concept to thicken sea ice or glacier top ice, and thus help reverse sea level rise, and assure freshwater security.

2 Uncertainty

The Glitter Belt concept is developed with calculations derived by applying known physical laws to a defined problem. Primary data come from the published literature.The effects of their stated uncertainties are considered below. For the concept presented in the paper, the primary uncertainty is whether enough upper bound space has been provided for cost and other requirements.

The Glitter Belt project seeks to create an architecture to solve one of the most difficult challenges facing Humanity, in an urgent manner. Work at the present stage is mostly about reducing uncertainty.

1. Overall Project Cost: We argue that in an architecture that is optimized to reflect light, the mass will be dominantly that of the reflector and its supporting structure. Thus, from the known cost per kilogram of Aluminized Mylar sheet (just over $3/kg in 2023), and the target weight per unit area of reflector (the Wing Loading of the Flying Leaf) a good estimate is derived for the marginal cost of additional Flying Leaf vehicles in the asymptotic limit as system size increases in full deployment. Flying Leaf vehicles weigh a maximum of 1.25 Newtons per square meter of reflector, and that costs $1.25/9.8 * 3 = \$0.38265$ per square meter. A Flying Leaf measuring $32 * 11 * 64 = 22528$ square meters should cost about $8620. From initial costing (retail prices) of Carbon Fiber structural components, motors and solar panels, there is no indication that this is a severe underestimate.
2. Overall Carbon Credit as Project Cost: However, we do not require accuracy of the above estimate. We calculate an equivalent Carbon Credit for reversal of EEI back to 1990 using the FL reflectors. The Climate Science community attributes the rise in EEI since 1990, to the accumulation of GHG in the atmosphere since 1990, which absorbs and retains heat. Thus, reversing EEI back to 1990 should be credited the same as removing the GHG accumulated since 1990. When this equivalence is calculated, it comes to just over 0.096 CEU per square meter of reflector deployed at 30k, altitude. FL attrition of 5% is already considered in this calculation. At a nominal expectation of $10 per CEU market value, the 22528 square meter FL considered above, earns $21,627. The total cost of all the FLs deployed, then becomes roughly $4.15 Trillion. As seen above, the actual cost may be only a third as much.
3. EEI: The target of net heating rate or EEI is based on the estimate from[1] as “0.87 +- 0.1". This is a 11.5% error to each side of the mean. We suspect that it is intended to convey a 10% error bound, but the answer from the published numbers is 0.97 W/m^2 as upper bound. The target is based on a measured average over the years from 2010 to 2018. We do not have data from 2018 to 2022, and there are indications that EEI has been going up. The average based on the years from 1971 to 2018 is only 0.47. Thus it is likely that the upper limit of EEI to be used is 0.97. However we use the given average figure of 0.87 because it appears to have held quite stable in recent years and we have no data upon which to base a higher average.
4. Wing Loading: There is uncertainty in the wing loading that can be achieved for the FL vehicles. We project that W/S should be less than 1.25 N/m^2, if profile drag coefficient is no higher than 0.025, to guarantee that FL vehicles stay above Controlled

Airspace (18288 meters above Mean Sea Level) through a 12-hour night. Laboratory experiments discussed in referenced papers including our own support the feasibility of achieving the 1.25 N/m^2 number even with present-day 1-MIL Mylar and Carbon Fiber truss structure. As thinner reflective sheets are put into use, the Wing Loading will decrease further. We believe the actual wing loading will be no higher than 1.0 N/m^2 and the profile drag coefficient no higher than 0.18.

5. Balancing wing loading and aspect ratio: Each FLT can carry up a 32m x 64m sheet, rolled up. The sheet may be extended in small increments, up to about 4 meters, to keep the Aspect Ratio of the FLT not lower than 4. Low value of W/S obtained by increasing the deployed area of reflective sheet, reduces the lift coefficient needed for a given speed and air density. However, Aspect ratio comes down as sheet chord increases. The Lift-Induced Drag Coefficient $C_{Di} = {C_L}^2/\pi AR$.

   Once the sheet-frames are joined to form an FL, the span is 352m. Chord can be increased to 32m and still have an Aspect Ratio of 11. Further, two FLs can be joined to form a span of 704m. This allows sheet chord to be fully unfurled to 64m, and still have an Aspect Ratio of 11. This doubles the area of previous designs used to arrive at the 1.25 target, without a corresponding increase in weight. Thus we can state that the upper bound of W/S is 1.25 N/m^2 and it can be achieved.
6. Profile drag coefficient of 0.025 is easily achieved, given present state of vehicle design for low-speed applications. Thus it is an upper bound. Flight simulation even of FLTs is giving values ranging near 0.015. FLs are lower.
7. Flight environment: Our calculations are based on the 1976 US Standard Atmosphere [2], which is also adopted as the ICAO International Standard Atmosphere. Temperature will vary from the average given. During the daytime there is sufficient power margin to accommodate higher temperature (lower density), and the FL vehicles have been tested successfully in simulation up to a standard altitude of 36 kilometers, providing enough certainty of operation. During the night, temperature is likely to be lower than the average, so that density is higher and the rate of descent lower. Thus our calculations based on the Standard Atmosphere are conservative. Maximum daytime temperature on exposed components such as motors is taken as 85 deg. Celsius (358K). This is based on estimates from the Webb Space Telescope, for temperatures reached on motors exposed to the Sun in Space at approximately the orbit of Earth around the Sun. This is conservative as there is cold air (217 K) flowing over the motors.
8. Wind data [3] have large variation and uncertainty; however there is large spatial variability as well.There is no requirement for FLs to follow a given path. They can drift East-West without affecting the Summer Follower requirement. North-south variability of winds is less than East-West. Away from the polar regions, high-altitude winds have only small North-South components, easily compensated by the FL's daytime propulsion, and by varying flight direction. The key requirement is for the FL to be able to fly at speeds that are high enough to avoid being blown far away from desired positions. This appears to be satisfied.

3 Gliding To Stay Above Controlled Airspace

3.1 Aerodynamics Method Level Required

All of the aerodynamics are in the incompressible flow regime - except for propellers. Propeller speeds expected to get into the high subsonic regime at high altitudes. Most of the vehicle and sheet surfaces will experience low-Reynolds Number boundary layers under cruise conditions, but may transition to turbulence in take-off conditions or while flying against winds.

Most operations are in the steady aerodynamics regime. Gust response may cause unsteadiness given low flight speeds.

Interaction (vortex generation/ flow separation) may be expected at wing/fin corners and fin/sheet corners. Must be minimized.

Some waviness of the sheet surface may be expected especially during gust encounters and perhaps in night-time descent.

Detailed wing and sheet loading may require a lifting-line formulation (high aspect ratio). Perhaps vortex-lattice methods.

3.2 Generalized Night-Time Glide Requirement

Ee will show a generalized estimation of what it takes to survive a night-time unpowered glide from 30.48 km, while staying about 18.8 km, above the edge of Class A Airspace, through 12 hours of darkness. Dawn powers the solar cells to restart the propellers. Since the Flying Leaf is intended as a Summer Follower craft, the longest night is when crossing the Equator and is no longer than 12 hours. In fact, at 30.48 km altitude, sunlight can be seen for some time after the sun has set as seen from ground level. Rays coming refracted through the atmosphere will continue to provide some power to the solar cells wrapped around the leading edges and lower front surface of the propelling wings. At dawn the vehicle is above18.8km altitude, high enough to enjoy a similar benefit in getting pre-dawn rays. Anywhere else other than the Equator, following the Summer Sun means the days are longer than the nights. So the 12-hour requirement is conservative.

From Figure 1, steady glide is a process where the aircraft is set with zero thrust, to a selected lift coefficient, and settles to a steady speed and descent rate for a given altitude. The attitude is held, and the speed decreases as altitude decreases and density increases. From the force balance shown in the Figure, along the horizontal axis, conservation of momentum gives

$$LSin(\theta) - DCos(\theta) = 0 \tag{1}$$

$$LCos(\theta) + DSin(\theta) - Mg = 0 \tag{2}$$

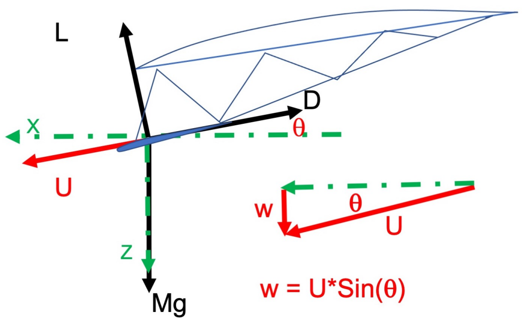

Figure 1: Steady Glide. Descent rate w is related to flight speed U as shown.

From the first equation,

$$D/L = Tan(\theta) \tag{3}$$

From the velocity diagram shown, the descent rate w is given by

$$w = USin(\theta) \tag{4}$$

or

$$w = USin(Tan^{-1}(D/L)) \tag{5}$$

3.3 Formulating the analysis to find the lowest point of 12-hour night-time glide

Let us suppose the weight is W and the lifting surface (mostly sheet) area is S. The Wing Loading is thus (W/S). As given above, $W/S = 0.8$. The 11 sheets joined together as given above, have an Aspect Ratio, $AR = \frac{b^2}{S}$ where b is the span, and S is the lifting surface planform area. Here $AR = 22$.

The drag of an aircraft is usually given as

$$D = qSC_D \tag{6}$$

where q is the dynamic pressure $0.5\rho U^2$, ρ being air density and U being freestream speed.

The drag coefficient can be split into a part independent of lift, and one that is induced by lift

$$C_D = C_{D0} + C_{Di} \tag{7}$$

C_D0 includes the profile drag due to flow separation around various items, and the skin friction drag. We can easily show that by keeping the sheet chord short enough that the

Reynolds number based on sheet chord and freestream speed and density is in the laminar regime, the skin friction is close to that on a smooth flat plate at angle of attack, the drag coefficient being given by the Blasius expression

$$C_{D0viscous} = \frac{2 * 1.328}{\sqrt{Re}} \tag{8}$$

, the 2 to account for both upper and lower surface of the sheet. This coefficient is very small, and its variation over the range of conditions that we consider, is neglected for the present. Instead we take a reasonable value for the profile drag coefficient based on small low-speed airplane data. This is generally around 0.02.

Note: The value of C_{D0} is one of the primary risks of this design. While very small values are theoretically possible, waviness in the sheet can increase it hugely. We will discuss the uncertainty in C_{D0} presently.

The coefficient of lift-induced drag is found as

$$C_{Di} = \frac{{C_L}^2}{\pi ARe} \tag{9}$$

The spanwise efficiency factor e is taken as 0.9, a conservative value for rectangular wings of high aspect ratio such as the Flying Leaf.

To survive the night, we want the slowest possible descent rate. The gliding descent rate is given as

$$w = USin(Tan^{-1}(D/L)) \tag{10}$$

where L/D is the lift to drag ratio, and is equal to $\frac{C_L}{C_D}$. Steady glide as we know, consists of tilting the flight path downwards just enough that the forward component of lift, as well of gravity, pull the vehicle forward against the drag, while the upward component of lift and drag balance the downward pull of gravity. To achieve the lowest possible descent rate, two things are needed: Slow flight speed, and high L/D. This is different from the condition for best glide speed, which aims to maximize the distance travelled in glide. Here, reducing speed is as important as achieving high L/D. Going to C_{Lmax}, the maximum lift coefficient, gives a lower descent rate than going to the Speed For Minimum Drag, which gives maximum L/D. Here we fix the maximum lift coefficient at 1.0, because the thin sheet, although cambered, is best not taken to a higher lift coefficient than that. In other words, we fix the lift coefficient at 1, which, for a given altitude, determines the flight speed immediately. This allows us to calculate the induced drag coefficient, L/D and descent rate directly.

An expression for density variation between 35km and 14km was constructed from the Digital Dutch 1976 International Standard Atmosphere, which yielded, with 0.1% accuracy:

$$\rho = 2.0787e^{-1.58306E-04H} \tag{11}$$

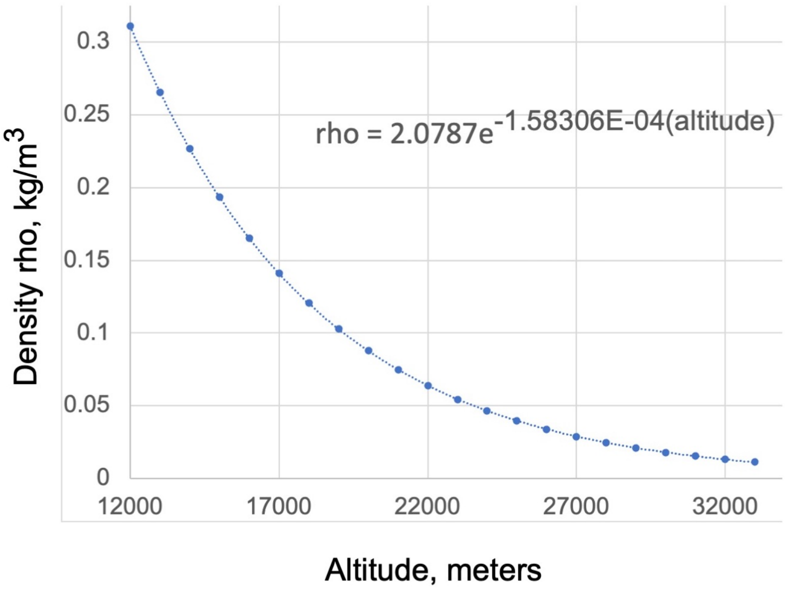

Figure 2: Empirical expression for variation of standard atmospheric density between 15000 and 35000 meters altitude. Based on the Digital Dutch calculator of the 1976 International Standard Atmosphere

where H is altitude in meters.

This is shown in Figure 2.

A simple calculation is now ready. At each altitude, the atmospheric density, W/S and C_L of 1 yield the flight speed U. This allows calculation of L/D and thus the sink rate. We chose a 250-meter descent step, with trapezoidal-rule calculation of the descent time. The first result shown is for a wing loading of $1.25N/m^2$, Aspect Ratio of 22 and C_{D0} of 0.2, in Figure 2

3.4 Range of Variation in Parameters

Figure 4 shows the tight range of parameters for the Flying Leaf to survive nighttime glide. We see that increasing the profile drag coefficient to 0.023 with a wing loading of $1.25N/m^2$ brings the Flying Leaf below 18.8km inside 12 hours, so it is not acceptable. On the other hand, decreasing the wing loading to $1.0N/m^2$ gives enough margin to increase profile drag coefficient somewhat.

The design space for a 30.48km (100,000 ft) cruise altitude, and the firm limit of 18.28 km (60,000 feet) as the edge of Class A controlled airspace, can be summarized by Figure 5. The 25-micron Aluminized Mylar sheet has an areal density of 50 grams per square meter, so that 0.1kg per square meter ($0.98N/m^2$) may be a practical current lower limit with this material and a carbon fiber support structure. We present $0.5N/m^2$ as a target lower limit of Wing Loading because solar sail technology now offers mass as low as 50 milligrams per square meter. The upper limit of wing loading is determined by varying

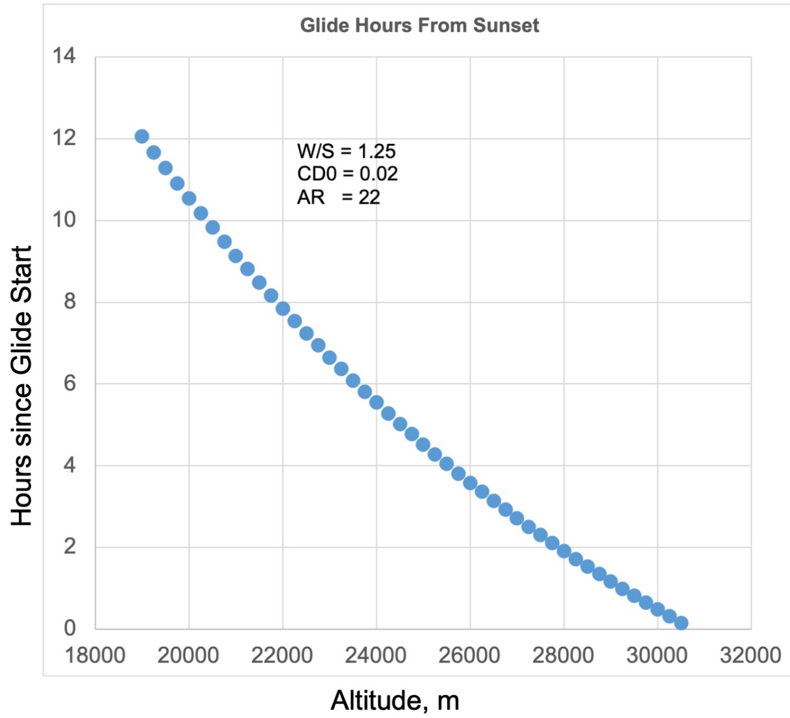

Figure 3: Night glide of the Flying Leaf with wing loading of $1.25 N/m^2$, Aspect Ratio 22 and profile drag coefficient of 0.02

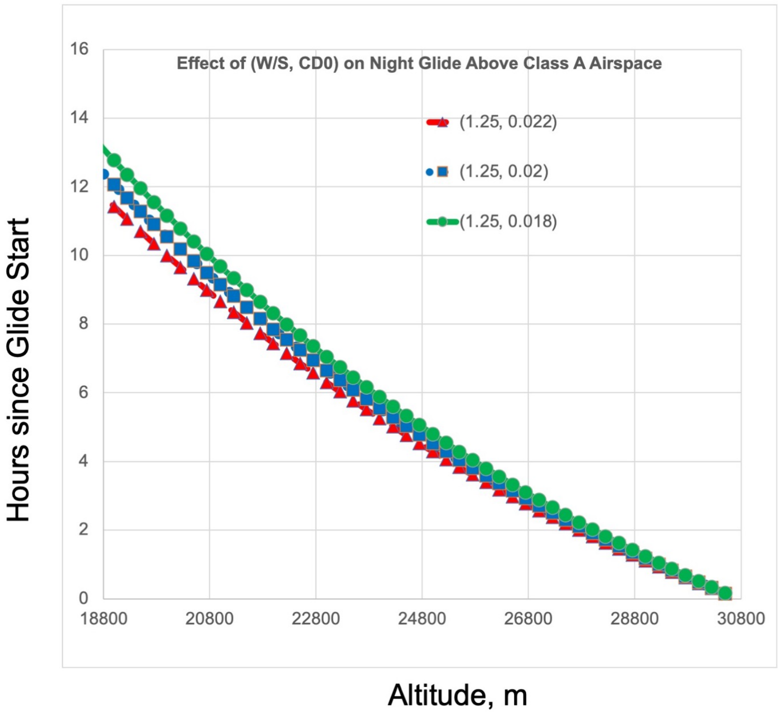

Figure 4: Effect of varying wing loading and profile drag coefficient, on night glide survival above 18.8km altitude

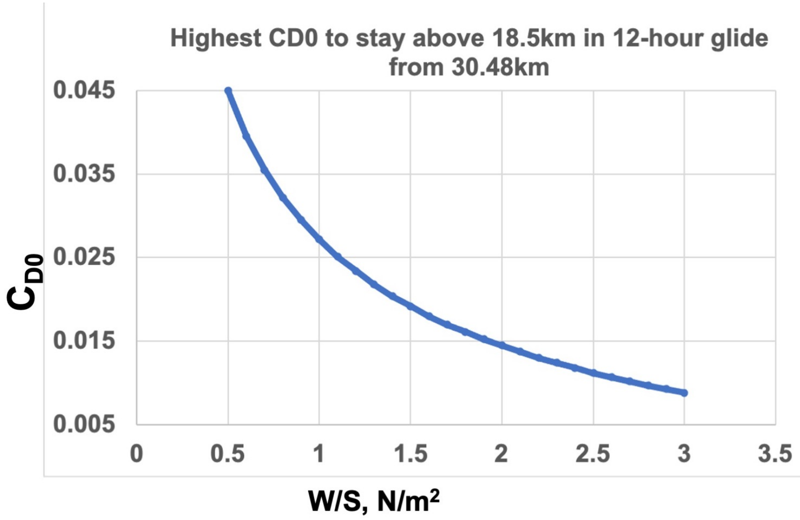

Figure 5: Limiting values of profile drag coefficient, for given choice of wing loading, to stay above 18.5km in 12-hour glide from 30.48km

C_{D0}: we do not see prospects of achieving C_{D0} below 0.01.

Another way to use higher wing loadings and profile drag coefficiens would be to increase the daytime cruise altitude as high as 36 kilometers (roughly 120,000 feet). This is left to future analysis, as the payload and hence the Wing Loading are dictated on the first day when the Flying Leaf is formed. The last Flying Leaflet to be attached, must reach the Leaf in time to be detached and descend to landing, while the Flying Leaf climbs up to 120,000 feet to start the glide at sunset. With careful logistics a 120,000 ft. altitude can be achieved, but at present we see no reason to explore that.

These considerations dictate selection of parameters for the Flying Leaf conceptual design. We choose nominal values of Wing Loading $W/S = 1.25N/m^2$, Profile Drag coefficient $C_{D0} = 0.02$, and 30.48 km cruise altitude. Daytime cruise will also be at lift coefficient of 1, because the high Aspect Ratio keeps the lift-induced drag coefficient C_{Di} very low. Optimal speed would be where $C_{Di} = C_{D0}$ but that would take the lift coefficient to dangerously high values for the thin sheets. If C_{D0} values come down much closer to the ideal values where only laminar-flow viscous drag matters, a better ideal cruise speed may be possible, but that requires proof of such C_{D0} in large-scale flight testing.

The calculation data are given below:

Table 1: Data for 12-hour glide. A simple step integration is done. A trapezoidal integration increases descent time by perhaps 15 minutes in 12 hours, so the present method is conservative without being excessively so.

Altitude in m	Density ρ	Speed u m/s	uSIN(ATAN(D/L))	Δ t sec	Glide hours
36576	0.006	30.73	0.908	275	0.08
35326	0.008	27.83	0.823	304	0.48
34076	0.009	25.21	0.745	335	0.93
32826	0.012	22.83	0.675	370	1.42
31576	0.014	20.68	0.611	409	1.97
30326	0.017	18.74	0.554	451	2.57
29076	0.021	16.97	0.502	498	3.24
27826	0.025	15.37	0.454	550	3.97
26576	0.031	13.92	0.412	607	4.78
24326	0.044	11.65	0.344	726	6.46
22076	0.063	9.75	0.288	867	8.47
20826	0.077	8.83	0.261	957	9.75
19576	0.094	8.00	0.237	1057	11.16
18826	0.106	7.54	0.223	1122	12.08

4 Reversing Global Warming To 1990

The calculation proceeds as follows. First the parameters and an estimate of total number needed just to cancel out net heat retention using the EEI (Earth's Energy Input) [1] as criterion.

1. Reflector area of a Flying Leaf (FL) vehicle is 11 times 32m span times 64 m chord. This assumes that 11 Flying Leaflet (FLT) vehicles take off and climb to 30.5km, where they rendezvous to form a single FL. FLT span is held down to 32m from our earlier choice of 64 m for ease of manufacture, transport logistics, and operations field choice. To keep aspect ratio moderate, these FLTs climb with their reflective sheet mostly retracted. For instance, at takeoff the FLT sheet is deployed only to 4 m chord, unrolled from the sheet roll at the front of the sheet-frame. During climb past the troposphere, the sheet is deployed more, to reduce wing loading. At rendezvous, since there is plenty of solar power to counter drag power due to induced drag, and the cruise lift coefficient is very low, the sheet is deployed to 32m.

   Once formed, the aspect ratio is high enough (11) to permit slow night-time glide. Once two FLs are assembled in proximity, they can fly close together and rendezvous at wing tips, to form a double FL, and then deploy the sheets to a full 64m. Thus the rolled up sheets at least with second-gen FLTs, will be 64 m chord when fully deployed. The sheet frames made of carbon truss will telescope from the 32m used at takeoff, to the full 64m. This also puts the control surfaces far back for better "tail volume" for stability and control.

   Nothing is different about the FLs when joined, except that aspect ratio remains at 11 even when sheets are fully deployed to 64m chord. Our generalized glide calculation assumes Aspect Ratio 11. We use the 11 x 32 x 64 sheet dimension to calculate reflection. Please see Table 2.
2. Reflector area effectiveness: The FL flies on a Peak Summer Follower trajectory, between the Tropics of Cancer (23.25 deg. North) and Tropic of Capricorn (23.25 deg. South). Every day it is at latitude where the local Sun traces a daytime trajectory bisecting the sky. We assume that the sheet is horizontal and thus presents an $A * Sin(Azimuth)$ area variation normal to the Sun where A is sheet area, approximated by the 45 degree value.
3. Average hours of sunlight per day increases from 12 at the Equator to 14 at the Tropics of Cancer and Capricorn. For simplicity we take the linear average. This is conservative as seen in the next step.
4. Only the sunshine between 30 degrees and 150 degrees measured from the horizon, is taken to be effectively reflected. This is because currently we do not have data on how InfraRed is reflected, below 30 degrees from the horizon. We do know [4] that at 30 degrees, fully 98.5% of IR is reflected. *Note: For the Polar Necklace project discussed later in the paper, we will have to modify strategy. Some form of the Quad-Frisbee discussed towards the end of the paper, may be needed to hold reflectors at a relatively shallow angle to the horizon.*
5. Combining the above items we arrive at the estimate of average 8.67 hours per day of full AM0 sunlight ($1367W/m^2$) reflection by the full area of the reflector.

6. The above is true every day of the year since the FL is always under the local Summer Solstice.
7. So we can arrive at the number of Joules reflected per FL per year.
8. Next we take the EEI of 0.87 W/m^2 of Earth's surface area, and estimate the total net heat added to Earth per year.
9. This directly gives the number of FLs that must be operating to cancel this out, as an architecture overview.
10. We add 5% to account for failures and retired FLs. Beyond the initial development stage, there is no reason for much attrition.
11. Note that the reflective sheet and sheet frame, including the front fairing, sheet-roller spar, side frame trusses, sheet and aft spar with control surfaces, are left with the FL upon rendezvous, and so the number of sheet-frames built must equal the number of launches. However the number of full FLTs needed is only 3/11 of the total number of launches, since only 3 out of 11 of the remaining parts of the FLT vehicles, are left attached to the FLs, while 8 out of 11 return to base to be fitted with new sheets and frames to carry up.
12. So we need less than 150 million FLTs, but over half a billion Sheets and Sheet-frames, and launches of all of them.

Table 2: Estimating total number of FLs and FLT launches to counter EEI.

Parameter	Value
Leaf Area 11*32*64	22528
Area effectiveness:	0.866025404
Av hrs/day due to Latitude variation (12 to 14)	13
Hours effective per day: 30 deg. To 30 deg.	8.67
Joules reflected per day (average)	8.27841E+11
Days in a year	365.25
Joules reflected per year/FL	3.02E+14
Total EEI W/m^2	0.87
Surface Area of Earth, m^2	5.10E+14
Heat added by Sun now	4.43E+14
Joules per year	1.40E+22
FLs needed	4.62E+07
No need for 2X since only 12hrs/day considered	
FLT launches at zero attrition	5.09E+08
Add 5% attrition	5.34E+08
# of FLTs built: Only need 3/11 as many FLTs as launches	1.46E+08
Sheet+roller+frame:	5.34E+08

Note that there is no intention, and fortunately no feasibility, to build and launch that many vehicles within a short period. The initial ones will be for testing and data collection. Subsequent versions will incorporate lessons. It takes time and funding to build manufacturing and launch facilities, and monitoring/data transmission centres. Given this reality it is logical to ask what can be gained from having such facilities operating for a long time. What is a reasonable project lifetime profile from start to finish?

This leads to the ambitious project to go much further and reverse Global Warming all the way back to 1990 (the original Kyoto goal) with no help from any other measures, whether GHG reduction, energy efficiency gains, reforestation or other Geo-Engineering projects. Again this is highly conservative: we certainly expect that as people realize that we can win, all such other projects will ramp up, at least to claim their share of Credits.

The process is as follows:

1. We assume 2024 start, since this is being written in January 2023. We have to get started sometime, and heat is building up at the EEI rate every second. We are currently racing to detail-engineer and build the first 8m FLT flight test vehicle, which will start reflecting sunlight when it comes out for launch. It is possible to have flight tests commencing within 3 to 6 months if there is determined progress. With the first test flight, the 16m flight test vehicle building can commence with flight test in another 2 months. As soon as that succeeds in reaching 30 km, high-altitude rendezvous, detachment and return to base, the first full-scale (32m span) FLT can be built and tested (another month or two), followed by the first 25 to build the first FLs. At that point FL build-deploy can commence and ramp up, to deploy the first 1100 before the end of 2024, with a fast ramp-up around the world following that.
2. The manufacturing-deployment rate is set, balancing the better design available with later deployment, the cost of overcoming delays in setting up manufacturing plants and hiring and training labor, etc. This process will require a detailed Multi-Disciplinary Design Optimization, considering other factors such as cost of borrowing funds, rate of disbursement, and in this case the health of national economies. For now it is set arbitrarily and iterated to minimize the needed numbers. Obviously, fastest ramp-up of deployment reduces the total number needed to reach the 1990 goal by 2055. A gradual wind-down minimizes the stress of reducing employees or transitioning facilities to other manufacturing.
3. There are two vehicle counts in Table 2. One is for the total number of launches which is also the number of sheets and sheet-frames launched. The other is of the monoplane parts of the FLTs built, which is only 3/11 of the sheet count. r
4. Each year we put in a number of FLTs to be built, and derive the number of assembled FLs in operation.
5. The Joules per year reflected by these FLs, all in Peak Summer Follower operation, is calculated.
6. The total heating per the EEI rate is calculated.
7. Net heating is the difference between the expected EEI heating, and what is reflected out by our FLs.
8. We use the EEI to estimate the heat level for each year.

9. As FLT production ramps up to the selected plateau, net heating becomes negative
10. Heating level rolls back in years.
11. We ramp down for a graceful exit of the Glitter Belt to reach 1990 level inside 30 years, our specified target.

4.1 Cancelling Out Today's EEI

In Table 3 please note that by the year 2041, we reach the cumulative heat level of 2023 again. In other words, we will have cancelled out the heat put in by today's heating rate. It took us that long because we could not have had 137 million FLs operating by the end of 2023 to suddenly cancel out the EEI, nor should we have tried because we need the years of continuous data and modeling to assure ourselves and the world that we would not be doing anything bad.
So this gives us the basis for calculating the equivalence of negating the effect of TODAY's GHG accumulation, which is what causes the 0.87 W/m^2 EEI. How long it took us, and how many square meters of reflector area we needed, are somewhat functions of our architecture: someone else might choose to do things differently.

This also raises some ominous warnings. The present ambitions described by international entities is reflected in the 2022 McKinsey Report [5].They estimate the cost to be $275 Trillion.

Calculation of Sunlight Reflection Credit The bases for our calculation are the estimate of the EEI [1], and a reasonably conservative estimate of the market price at $10 per 1 CEU (Carbon Emission Unit) or 1 Metric Ton of CO2 removed from the atmosphere.

Von Shuckmann *et al* [1] also specifies that to cancel out the EEI at today's level of heat, one would have to reduce the concentration of CO2, from 410 PPM to 353 PPM. This is a difference of 57PPM. However that is only CO2.

Figure 6 from [6] includes total GHG concentration including aerosols in the atmosphere from 1860 to 2023. It shows that the 2020 level is gas 465PPM. The accompanying article cites an annual rate of increase of 4.7ppm. We extrapolate to 2023, dropping one year because of the COVID-19 related economic slowdown. This gives a 2023 level of 465+9.4 = 474.4. Figure 7 shows data from [7]. We estimate the 1990 level from the figure to be 412, given a difference of 62PPM.

The conversion of PPM of CO2 to Gigatons (7.82GT per PPM) [8], gives 484.84GT of CO2 equivalent. A valuation of USD 10 per CEU we readily arrive at a creditable value for equivalent sunlight reduction.
By summing up the total sheet area launched until 2055, we can establish the equivalence, which is valid for our architecture. This is shown below in Table 4. The result is an equivalence of 0.1122 CEUs per square meter of our reflectors. At 10 US dollars per CEU, the Carbon Credit equivalent Solar Reflection Credit is $1.12 per square meter of reflector.
The total CEU cost works out to USD 4.85 Trillion, to reduce roll Global Warming back to the level of 1990.

Table 3: Calculating Glitter Belt Operation To Reverse Global Warming from 2024 to 1990

Year	FLTs, M	Sheets Built,M	FLs, M	Reflect Area	Heat Refl, J	Net Heat, J.	Cum. Joules	Heat Level of Yr
2024	0.001	0.004	0.003	7.8E+06	1.0E+17	1.4E+22	1.4E+22	2024
2025	0.01	0.004	0.004	8.6E+07	1.2E+18	1.4E+22	2.8E+22	2025
2026	0.05	0.2	0.021	4.8E+08	6.4E+18	1.4E+22	4.2E+22	2026
2027	0.55	2.0	0.195	4.4E+09	5.9E+19	1.4E+22	5.6E+22	2027
2028	5.5	20	1.9	4.3E+10	5.8E+20	1.3E+22	7.0E+22	2028
2029	32.9	120	12	2.8E+11	3.7E+21	1.0E+22	8.3E+22	2029
2030	32.9	120	23	5.1E+11	6.9E+21	7.1E+21	9.3E+22	2030
2031	32.9	120	33	7.5E+11	1.0E+22	4.0E+21	1.0E+23	2030
2032	32.9	120	44	9.8E+11	1.3E+22	8.2E+20	1.0E+23	2030
2033	32.9	120	54	1.2E+12	1.6E+22	-2.3E+21	1.1E+23	2031
2034	32.9	120	64	1.4E+12	1.9E+22	-5.5E+21	1.0E+23	2030
2035	32.9	120	75	1.7E+12	2.3E+22	-8.6E+21	9.8E+22	2030
2036	32.9	120	85	1.9E+12	2.6E+22	-1.2E+22	8.9E+22	2029
2037	32.9	120	96	2.2E+12	2.9E+22	-1.5E+22	7.7E+22	2029
2038	32.9	120	106	2.4E+12	3.2E+22	-1.8E+22	6.2E+22	2027
2039	32.9	120	116	2.6E+12	3.5E+22	-2.1E+22	4.4E+22	2026
2040	32.9	120	127	2.9E+12	3.8E+22	-2.4E+22	2.3E+22	2025
2041	32.9	120	137	3.1E+12	4.1E+22	-2.7E+22	-1.3E+21	2023
2042	32.9	120	148	3.3E+12	4.5E+22	-3.1E+22	-2.9E+22	2021
2043	32.9	120	158	3.6E+12	4.8E+22	-3.4E+22	-5.9E+22	2019
2044	27.9	102	167	3.8E+12	5.0E+22	-3.6E+22	-9.3E+22	2016
2045	23.7	87	174	3.9E+12	5.3E+22	-3.9E+22	-1.3E+23	2014
2046	14.2	52	179	4.0E+12	5.4E+22	-4.0E+22	-1.7E+23	2011
2047	5.7	21	181	4.1E+12	5.5E+22	-4.1E+22	-2.1E+23	2008
2048	3.4	13	182	4.1E+12	5.5E+22	-4.1E+22	-2.5E+23	2005
2049	1.2	4	182	4.1E+12	5.5E+22	-4.1E+22	-2.9E+23	2002
2050	0.419	2	182	4.1E+12	5.5E+22	-4.1E+22	-3.3E+23	1999
2051	0.105	0.38	182	4.1E+12	5.5E+22	-4.1E+22	-3.7E+23	1996
2052	0.026	0.10	182	4.1E+12	5.5E+22	-4.1E+22	-4.1E+23	1993
2053	0.003	0.01	182	4.1E+12	5.5E+22	-4.1E+22	-4.5E+23	1990

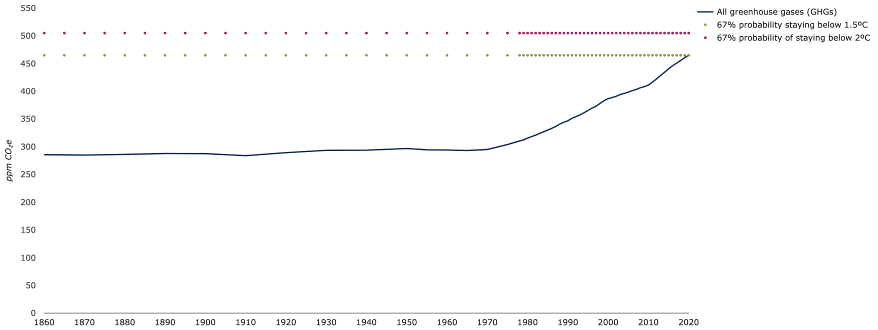

Figure 6: Total GHG increase, 1860 to 2020. Data from [6].

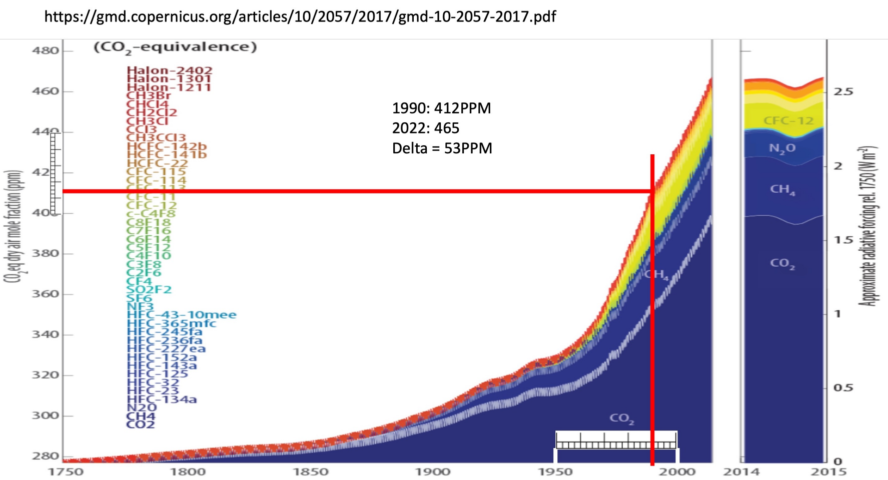

Figure 7: Total GHG increase. Data from [7].

Table 4: Constructing an equivalence between Carbon Dioxide removal and heat reflection using data from [1], in zeroing out EEI at 2023 heat level.

2020 EEI, W/m^2	0.87	Value in US dollars of 1 CEU	10
Net reduction needed (474 to 412), PPM	62	GT CO2 equivalent at 7.62GT per PPM	48
Total sheets to be launched to reach 1990	2.11E+09	Total sheet area, sq.m	4.3
Total Credit, $	4.85E+12	CEU per sq.m	0.1

If the GB project can be accomplished under this value, it is totally self-sustaining. However, if the project also manages to reverse the loss of mountain glacier snow cover, and strengthens the sea ice band surrounding the coast of Antarctica to inhibit sea wave erosion under the large ice ledges, we may be able to reverse sea level rise, and replenish freshwater supplies. A monetary value on that would be easy to see but very hard to estimate, and decide who should pay that value. Even if a glacier that is entirely inside one nation is to be shielded, that would have to be subjected to the same rigorous validation as for geo-engineering applied anywhere else. Likewise the cost should be borne by all. Technology to do such missions will be drawn from the Polar Necklace mission. The Consortium structure is the only one we can imagine, to handle such global issues.

5 Reversing Sea Level Rise and Mountain Glacier Attrition

5.1 Polar Necklace Calculation

The Antarctic coastline has ice coming down to the beach in most parts, with a surface layer of sea ice extending out into the ocean. Some researchers say that the sea ice is disappearing for instance in 2022, while others say that it is growing. One theory holds that thinning sea ice becomes brittle under the heaving of water caused by wave action. When the sea ice cracks, it cannot strongly dampen the wave action as it penetrates beneath the overhanging ice shelves at the end of glaciers. Glacier flow accelerates if the sea ice cracks. The overhanging glacier edge shelf can also crack if storm-driven wave action is allowed to reach under the shelf undamped.

A practical key to ending the disintegration of ice shelves appears to be in strengthening the sea ice. If the delicate balance between winter snow and ice accumulation, and summer melting, were to be altered in favor of accumulation , the sea ice would thicken and get stronger. A strong sea ice band would keep more glacier snow from falling into saltwater. The net result may be a steady accumulation of ice [9, 10] on Antarctica, that significantly captures water and keeps it from fueling sea level rise.

Here we have calculated what it may take to remove the latent heat of fusion in the summer, corresponding to a 1mm thick layer of ice forming each year. Of course all these are to be verified by meteorological flight testing continuously,

Parameter	Value
Antarctic coastline, m	2.03E+07
Area of 1km wide strip, m^2	2.03E+10
Volume of layer 1mm thick	2.03E+07
Mass kg	2.03E+10
Latent heat needed, Joules in3 mo.	6.80E+15
Joules per day	7.56E+13
Sun Inclination: degrees	30
Correction Factor Sin 30	0.5
Joules Per FL per day, 12 effective hrs	9.97783E+11
Corrected for 30 deg. Azimuth	4.98892E+11
Corrected to 60% of AM1/AM0	2.18972E+11
FLs needed	3.45E+02

References

[1] Karina Von Schuckmann et al. “Heat stored in the Earth system: where does the energy go?” In: *Earth System Science Data* 12.3 (2020), pp. 2013–2041.

[2] Anon. NOAA. “US Standard Atmosphere 1976”. In: *Washington, DC: US Govtern-ment Printing Office* NOAA-S/T76-1562 (1976).

[3] Cameron Becario. *Earth: A Global Map of Wind, Weather and Ocean Conditions*. GF-S/NCEP/US National Weather Service. 2022.

[4] D McNulty. “Reflectivity Measurements”. MA thesis. Idaho State University, 2016. URL: `%7Bhttps://www2.cose.isu.edu/~mcnudust/publication/presentations/%7D`.

[5] Gautam Kumra and Jonathan Woetzel. “What it will cost to get to net-zero”. In: *The Business Times* (Jan. 2022).

[6] Anon Europa. *Atmospheric greenhouse gas concentrations*. Jan. 2023. URL: `https://www.eea.europa.eu/ims/atmospheric-greenhouse-gas-concentrations`.

[7] Malte Meinshausen et al. “Historical greenhouse gas concentrations for climate modelling (CMIP6)”. In: *Geoscientific Model Development* 10.5 (2017), pp. 2057–2116.

[8] Anon. *Conversion Tables. Carbon Dioxide Information Analysis Center*. Tech. rep. Oak Ridge National Laboratory, US Govt., July 2020.

[9] Johannes Feldmann, Anders Levermann, and Matthias Mengel. “Stabilizing the West Antarctic Ice Sheet by surface mass deposition”. In: *Science advances* 5.7 (2019), eaaw4132.

[10] Ted A Scambos et al. “The link between climate warming and break-up of ice shelves in the Antarctic Peninsula”. In: *Journal of Glaciology* 46.154 (2000), pp. 516–530.